

3-30-2004

# A study of hydraulic properties of high level waste simulant

Sudhakar N. Chodavarapu  
*Florida International University*

**DOI:** 10.25148/etd.FI14060814

Follow this and additional works at: <https://digitalcommons.fiu.edu/etd>

 Part of the [Civil Engineering Commons](#)

---

## Recommended Citation

Chodavarapu, Sudhakar N., "A study of hydraulic properties of high level waste simulant" (2004). *FIU Electronic Theses and Dissertations*. 2344.

<https://digitalcommons.fiu.edu/etd/2344>

This work is brought to you for free and open access by the University Graduate School at FIU Digital Commons. It has been accepted for inclusion in FIU Electronic Theses and Dissertations by an authorized administrator of FIU Digital Commons. For more information, please contact [dcc@fiu.edu](mailto:dcc@fiu.edu).

FLORIDA INTERNATIONAL UNIVERSITY

Miami, Florida

A STUDY OF HYDRAULIC PROPERTIES OF HIGH LEVEL WASTE SIMULANT

A thesis submitted in partial fulfillment of the

requirements for the degree of

MASTER OF SCIENCE

in

CIVIL ENGINEERING

by

Sudhakar N. Chodavarapu

2004

To: Dean Vish Prasad  
College of Engineering

This thesis, written by Sudhakar N. Chodavarapu, and entitled A Study of Hydraulic Properties of High Level Waste Simulant, having been approved in respect to style and intellectual content, is referred to you for judgment.

We have read this thesis and recommend that it be approved.

Georgio Tachiev

Rajiv Srivastava

Shonali Laha, Major Professor

Date of Defense: March 30, 2004

The thesis of Sudhakar N. Chodavarapu is approved.

Dean Vish Prasad  
College of Engineering

Dean Douglas Wartzok  
University Graduate School

Florida International University, 2004

## DEDICATION

I dedicate this thesis to my family. Without my patience, understanding, support, the completion of this work would not have been possible.

## ACKNOWLEDGMENTS

I would like to thank my committee members for their support and patience. First I would like to express my gratitude to Dr. Rajiv Srivastava for his support in completing the thesis work. Secondly I thank Dr. Shonali Laha for her perusal of the manuscript and unwavering attention to detail. Finally I would like to thank Dr. Georgio Tachiev for his support from the beginning in completing the experiment, writing the report and his continual availability.

## ABSTRACT OF THE THESIS

### A STUDY OF HYDRAULIC PROPERTIES OF HIGH LEVEL WASTE SIMULANT

by

Sudhakar N. Chodavarapu

Florida International University, 2004

Miami, Florida

Professor Shonali Laha, Major Professor

The purpose of this study was to determine the unsaturated hydraulic properties of High Level Waste simulant by applying inverse modeling and parameter estimation methods and data obtained by experiments.

Saltcake simulant was placed in column equipped with tensiometers and flow meters. Variable pressure boundary conditions ranging from 100 to 500 cm were applied along the column, outflow and the pressure head were measured with respect to time. The experimental data was analyzed using an inverse modeling software and the van Genuchten's hydraulic parameters for unsaturated porous media were determined. In addition, the unsaturated hydraulic conductivities were obtained as a function of the moisture content. Hydraulic conductivities ranged from  $5.36E-5$  to  $4.29E-2$  cm/hr. The data was analyzed to determine the percentage reduction in storage capacity as a function of applied pressure. The experimental results were compared with output from direct simulations of interstitial fluid drainage from a column and showed good agreement.

While there are several studies on determining the saturated hydraulic conductivities, this work demonstrates that the van Genuchten unsaturated model is a valid model and can be applied for three dimensional modeling and for determining the level of separation of radioactive waste (Cs 137) using interstitial fluid drainage.

## TABLE OF CONTENTS

CHAPTER	PAGE
1	INTRODUCTION ..... 1
2	GOVERNING EQUATIONS..... 5
	2.1 MASS BALANCE..... 6
	2.2 DARCY’S LAW ..... 6
	2.3 CONSTITUTIVE RELATIONS OF UNSATURATED FLOW ..... 8
	2.4 RICHARDS EQUATION ..... 9
	2.5 INITIAL AND BOUNDARY CONDITIONS ..... 12
	2.5.1 Boundary Conditions: ..... 12
3	LITERATURE REVIEW ..... 14
	3.1 EXPERIMENTAL METHODS ..... 15
	3.1.1 Determining the hydraulic conductivity of the soil by means of field scale drainage model ..... 16
	3.1.2 Analysis of Unsaturated water flow in a large sand tank..... 16
	3.2 PARAMETER ESTIMATION..... 18
	3.2.1 Predicting unsaturated hydraulic conductivity of porous media based on the physical properties ..... 19
	3.2.2 Assessment of the hydraulic characteristics of unsaturated base- course materials ..... 21
	3.2.3 Parameter Estimation and Identifiability Analysis ..... 24
	3.2.4 Inverse determination of unsaturated hydraulic parameters ..... 24
4	CONDUCTIVITY OF POROUS MEDIA ..... 27
	4.1 MULTIPHASE FLOW IN POROUS MEDIA ..... 28
5	MATERIALS AND METHODS..... 30
	5.1 EQUIPMENT..... 31
	5.1.1 Tensiometer..... 31
	5.1.2 Pressure Transducer ..... 32
	5.1.3 Vacuum Hand Pump ..... 34
	5.1.4 Pressure Regulator ..... 35
	5.2 DATA ACQUISITION ..... 36
	5.3 SALTBED SIMULANT PREPARATION ..... 37
	5.3.1 Saltcake composition ..... 37
	5.3.2 Steps in preparation of the saltcake simulant..... 38
6	RESULTS AND DISCUSSIONS..... 41
	6.1 PRESSURE HEAD ..... 42

6.2	CUMULATIVE OUTFLOW .....	44
6.3	MOISTURE CONTENT .....	46
6.4	HYDRAULIC PARAMETERS .....	48
6.4.1	Parameter Optimization .....	48
6.5	HYDRAULIC CONDUCTIVITY .....	50
6.6	DIRECT ANALYSIS USING INVERSE OPTIMIZED PARAMETERS .....	54
6.7	ESTIMATED VOLUME OF INTERSTITIAL FLUID FROM DRAINAGE.....	58
7	CONCLUSIONS.....	61
7.1	CONCLUSIONS.....	62
7.2	RECOMMENDATIONS.....	62
	REFERENCES .....	63



## LIST OF TABLES

TABLE	PAGE
1. Average Values of Van Genuchten Model soil hydraulic parameters for major soil textural groups according to (Van Genuchten, 2000).....	18
2. Saltcake simulant chemicals .....	37
3. Average moisture content obtained from the experimental data .....	48
4. Comparison of parameters .....	49
5. Comparison of average moisture content from inverse parameters and from experiment.....	56
6. Percentages of drained interstitial fluid from the tank.....	59

## LIST OF FIGURES

FIGURE	PAGE
1. Tensiometer with Ceramic Porous cup .....	32
2. Pressure transducer .....	32
3. Tensiometer attached to the pressure transducer .....	34
4. Pressure Controller.....	35
5. National Instruments data acquisition hardware.....	35
6. Experimental Setup.....	40
7. Measured and optimized cumulative bottom flux .....	43
8. Comparison of outflow rate and cumulative outflow .....	45
9. Moisture content variation with time.....	47
10. Variation of Hydraulic conductivity with time.....	51
11. Variation of average hydraulic conductivity with time .....	53
12. Cumulative Outflow comparison of direct analysis with inverse parameters with inverse analysis .....	55
13. Moisture content comparison from Experimental and inverse analysis .....	57
14 Increase of drainage percentage with increased pressure .....	60

## LIST OF VARIABLES

$\rho$	Density of the Phase [kg/m <sup>3</sup> ]
$\phi$	Porosity [-]
$\theta$	Volumetric Water Content [-]
$\theta_a$	Air content [-]
$\theta_w$	Water content [-]
$\mu$	Dynamic Viscosity [kg/m.sec]
$\rho_w$	Density of water at standard temperature and pressure [kg/m <sup>3</sup> ]
$\rho_a$	Density of air [kg/m <sup>3</sup> ]
$\theta_s$	Saturated water content [-]
$\theta_r$	Residual water content [-]
$\alpha$	Inverse air entry value [1/cm] (Van Genuchten Parameter)
$n$	Pore-size distribution index [-] (Van Genuchten Parameter)
$S_e$	Normalized water content [-]
$q$	Volumetric flux [m/s]
$k$	Intrinsic Permeability
$k_r$	Relative permeability
$K$	Unsaturated hydraulic conductivity [m/s]
$K_S$	Saturated hydraulic conductivity [m/s]
$p$	fluid pressure of phase [psi]
$p_a$	air pressure [psi]
$p_w$	Pressure of water [psi]
$p_c$	Capillary pressure [m]
$h_c$	Capillary pressure head [m]
$A$	Angle between direction of flow and horizontal direction [-]
$l$	Pore connectivity factor [-]
$d_{10}$	Diameter of the soil particles at 10% of cumulative grain size distribution [cm]
$\rho_b$	Bulk density [kg/m <sup>3</sup> ]
$\rho_s$	Particle density [kg/m <sup>3</sup> ]
$V_t$	Total volume occupied by the soil [m <sup>3</sup> ]
$V_{sc}$	Volume of voids in coarse-grained soil [m <sup>3</sup> ]

# 1 Introduction

The Savannah River Site (SRS) has 51 tanks containing about 30 million gallons of high-level waste (HLW) from nuclear fuel reprocessing. Each tank contains varying amounts of three types of waste, i.e., sludge, saltcake and salt solution. Sludge is insoluble and has settled to the bottom of the tank. Sludge is only eight percent of the SRS waste volume and has been estimated to be eleven million liters (Edwards et al 2002). The chemical composition of the sludge includes high levels of radioactive elements including strontium, plutonium and uranium mostly as hydroxides under very high pH. The remaining ninety two percent of the SRS waste volume is salt waste. The interstitial fluid may have high concentrations of cesium-137 and trace amounts of other radioactive elements in the form of dissolved salts and it is considered as HLW. Saltcake is the low-level tank waste that consists primarily of sodium nitrate or nitrite crystals that resulted from removal of water from previously neutralized waste supernatant liquid. The waste that was stored in the underground storage tanks needs disposition because several storage tank leakages occurred in the past at Hanford site<sup>1</sup>

The waste is stored in single shell and double shell storage tanks. DOE's single shell tanks (SST) are potential environmental hazards because only a single barrier contains the liquids and any breach in the barrier may cause contaminant spillage (Ramirez et al 1996). In addition, the lifetime of the SST has been exceeded, therefore, retrieval within the shortest time span is essential to prevent an environmental catastrophe. To prevent the potential catastrophe and to reduce associated human health

---

<sup>1</sup><http://www.hanford.gov/press/1997/97-104.htm>

and safety risks DOE plans to process these wastes for final disposition. The removal of HLW costs hundreds of millions of dollars and will require over twenty years to accomplish (Noyes et al 2003). DOE is investigating alternative methods and technologies for HLW removal and processing, which include dissolution of high level salts and supernatant drainage to separate the high activity components. Interstitial fluid displacement by uncontaminated water has been suggested for preferential retrieval of Cs-137 and consequent treatment of the waste (Staheli and Peters, 1998).

The radionuclide present at highest concentration in the underground storage tanks is cesium-137. Most of the high level waste will be present in the interstitial fluid and low-level waste in saltcake and sludge. Due to the porous nature of the saltcake and cesium concentration being very much lower than saturation, most of the cesium-137 exists only in interstitial fluid (Brooke et al 1999). It can be removed from the saltcake by displacing the contaminated interstitial liquid with uncontaminated liquid. Removing 70 to 90 percent of the interstitial fluid removes an equivalent percent of cesium and other soluble radionuclides (Suggs et al 2002).

The waste removal process should be demonstrated experimentally before implementing at the site. Laboratory experiments were conducted on the saltcake simulant that was prepared using different types sodium salts with similar porosity and capillary pressure as that of the high-level waste at the site. To determine the hydraulic properties of the saltcake an analogy of soil water in the vadose zone was used as reference. A number of well-established mathematical models were developed to determine the hydraulic properties of water in the soil. Experimental models developed

by van Genuchten (1980), Mualem and Richards (1964) have been used as the basis to estimate the unsaturated hydraulic conductivity of the saltcake. These models were developed using different types of soils of varied porosities and capillary pressures. Laboratory experiments were conducted on these soils and mathematical relationships were developed to determine hydraulic properties of the porous media. Because saltcake has a similar porous nature, we conducted similar experiments with synthetic saltcake and used similar mathematical relationships to determine hydraulic properties of the saltcake.

## **2 Governing Equations**



The following sections present the governing equations used to describe flow through unsaturated porous media. These equations were developed from mass balance and hydrological models.

## 2.1 Mass Balance

The mass balance equation includes two coupled equations for each phase (Bear 1979):

$$\frac{\partial}{\partial t}(\rho\theta) + \nabla \cdot (\rho q) = F \quad 1$$

where  $\rho$  = density of phase ( $\text{kg/m}^3$ ),  $q$  =volumetric flux (or Darcy flux) (m/d),  $F$  = source or sink of fluid ( $\text{kg/m}^3 \cdot \text{d}$ ),  $\theta$  = volumetric fluid content (dimensionless)  $\frac{\partial}{\partial t}(\rho\theta)$  is change of mass in a control volume in time,  $\nabla \cdot (\rho q)$  is divergence of mass flux in that volume. The porosity of the fluid can be defined as:

$$\theta_a + \theta_w = \phi \quad 2$$

where  $\theta_a$  = air content,  $\theta_w$  = water content, and  $\phi$  = porosity

## 2.2 Darcy's Law

Darcy's Law describes the relation between the flux and the individual phase pressures. From the momentum balance equations, generalized multiphase Darcy's law may be expressed as:

$$q = -\frac{kk_r}{\mu}(\nabla p - \rho g) \quad 3$$

Where,  $k$  = intrinsic permeability tensor of the medium ( $m^2$ ),  $k_r$  = relative permeability of fluid  $\mu$ =dynamic viscosity of fluid (kg/m.d),  $p$  = fluid pressure of phase (kg/m.d<sup>2</sup>),  $g$  = acceleration due to gravity vector (m/d<sup>2</sup>)

The pressure head is defined as

$$h = \frac{p_a}{\rho_w g} \quad 4$$

The relation between the permeability and non-linear conductivity tensor is given by:

$$K = \frac{\rho_w g k k_r}{\mu} = K_s k_r \quad 5$$

Where,  $\rho_w$  = density of water at standard temperature and pressure (kg/m<sup>3</sup>),  $K_s$  = conductivity when the porous medium is saturated with fluid.

From Equations 3 and 4 Darcy's law can be written as

$$q = -K(\nabla h - \frac{\rho_a}{\rho_w} \mathbf{i}_z) \quad 6$$

$\mathbf{i}_z$  = unit normal oriented downwards in the direction of the force of gravity,  $\rho_a$  is the density of air.

The average flow velocity is defined as:

$$v = \frac{q}{\theta} \quad 7$$

Where  $v$  = flow velocity (m/d),  $q$ = volumetric flux.

## 2.3 Constitutive Relations of Unsaturated Flow

Equations 1 and 3 describe the flow conditions in the system. There are several unknowns in these equations. In order to close the system constitutive relations that relate the unknowns must be specified. The solution of equations 1 and 3 require knowledge of three constitutive relations pressure-saturation, relative permeability-saturation, and density-pressure are required (Binning 1994). The fluid saturation is a function of the difference between the pressures of the two fluids in the porous medium. The pressure difference is called the capillary pressure ( $p_c$ ) and is defined as:

$$p_c = p_a - p_w \quad 8$$

Where  $p_a$  = pressure of air or non-wetting phase,  $p_w$ = pressure of water or wetting phase,  $p_c$  = capillary pressure, with corresponding definition for the capillary pressure head ( $h_c$ ):

$$h_c = h_a - h_w \quad 9$$

One of the most commonly used functional forms to describe the pressure-saturation relation is that of van Genuchten (1980):

$$\theta = \frac{\theta_s - \theta_r}{(1 + (\alpha h_c)^n)^{\frac{1}{n}}} + \theta_r \quad 10$$

$\theta_s, \theta_r, \alpha, n$  are used as fitting parameters with a given set of capillary pressure saturation data.  $\theta_s, \theta_r$  are saturated water content and residual water content respectively,  $\alpha$  is the inverse of the air-entry value or bubbling pressure [1/cm],  $n$  is the pore size distribution index.

$$S_e = \frac{1}{[1 + (\alpha h)^n]^m} \quad 11$$

Where  $\alpha, n, m$  are van Genuchten's empirical constants affecting the shape of the retention curve,  $S_e$  is the normalized water content.

## 2.4 Richards Equation

The governing equation for the two-dimensional Darcian water flow in a variably saturated rigid isotropic porous medium is given in the following form of the Richard's equation:

$$\frac{\partial \theta}{\partial t} = -\frac{\partial q}{\partial z} = \frac{\partial}{\partial z} \left[ K \frac{\partial H}{\partial z} \right] = \frac{\partial}{\partial z} \left[ K \frac{\partial(-z-h)}{\partial z} \right] = -\frac{\partial}{\partial z} \left[ K \frac{\partial h}{\partial z} + K \right] \quad 12$$

The functional form given above ignores the effects of hysteresis. For more general drainage problems it may be useful to include hysteresis. Several computational models have been developed by other authors including Kool and Parker (1987), and

Moridis and Reddell (1991) who proposed a secondary water recovery system based on model results of unsaturated zone hysteresis.

The relative permeability is a function of fluid saturation, defined as

$$k_r(\theta) = S_e^{1/2} (1 - (1 - S_e^{1/m})^m)^2 \quad 13$$

where  $m = 1 - 1/n$ ,  $S_e$  = normalized water content

$$S_e = \frac{\theta - \theta_r}{\theta_s - \theta_r} \quad 14$$

The governing 1-D partial differential equation for water movement in unsaturated zone can be transformed to:

$$\frac{\partial \theta}{\partial t} = \frac{\partial}{\partial x} \left[ K \left( \frac{\partial h}{\partial x} \right) - \sin(A) \right] \quad 15$$

where  $\theta = \theta(h)$  is the volumetric water content,  $h = h(x, t)$  is the matrix potential,  $x$  is the position coordinate parallel to the direction of flow;  $t$  is the time;  $\sin(A)$  is the sine of the angle  $A$  between the direction of flow and the horizontal direction;  $K(h)$  is the hydraulic conductivity of the soil at matric potential  $h$ . An angle  $A$  of zero degrees corresponds to horizontal flow with  $x$  increasing from left to right; an angle of 90 degrees corresponds to vertical flow with  $x$  increasing in the downward direction.

The nonlinear relationships near saturation can affect the performance of numerical solution of Richard's equation in terms of accuracy and stability.

$$\frac{\partial \theta}{\partial t} = \frac{\partial}{\partial z} \left[ K \frac{\partial h}{\partial z} - K \right] \quad 16$$

The predictive Mualem model for the hydraulic conductivity function may be written as

$$K(S_e) = K_s S_e^l \left[ \frac{f(S_e)}{f(1)} \right]^2 \quad 17$$

with

$$f(S_e) = \int_0^{S_e} \frac{1}{h(x)} dx \quad 18$$

where  $K$  is the unsaturated hydraulic conductivity,  $K_s$  is the saturated hydraulic conductivity,  $l$  is the pore connectivity parameter usually assumed to be 0.5, and  $S_e$  the effective saturation given by Equation 14

$$\theta = \theta_r + \frac{\theta_s - \theta_r}{[1 + (\alpha h)^n]^m} \quad \text{for } h < 0 \quad 19$$

$$\theta = \theta_s \quad \text{for } h \geq 0 \quad 20$$

$$K = K_s S_e^l \left[ 1 - (1 - S_e^{1/m})^m \right]^2 \quad 21$$

where  $\theta_r$  and  $\theta_s$  are the residual and saturated water contents, respectively and in which  $n$  and  $\alpha$  are empirical shape parameters with  $m = 1-1/n$ .

## 2.5 Initial and Boundary Conditions

The solution of equation 12 requires knowledge of the initial distribution of the pressure head within the flow domain:

$$h(x,t) = h_i(x) \quad t=t_0 \quad 22$$

where  $h_i$  is a function of  $x$ ,  $t_0$  is the time when the simulation begins.

### 2.5.1 Boundary Conditions:

The coefficients in the above equation characterize the hydraulic properties of the medium: fluid retention  $\theta(h)$  and hydraulic conductivity  $K(h)$  (m/s). These functions are monotone increasing and constant in the saturated region ( $h \geq 0$ ), Soil columns are suitable and frequently used method to determine the hydraulic retention. Column experiments exhibit a flow regime only in one direction constituting a spatially one-dimensional model.

The experiments involve draining a vertically oriented soil column of fixed length with known initial pressure head distribution  $h(x)$  near saturation by slowly decreasing the pressure head  $h(t)$  at the lower boundary. Mathematically this is modeled by Dirichlet boundary condition. The flux at the upper boundary is adjusted to  $q=0$ , therefore a homogeneous boundary condition is used. The flux  $f(t)$  is measured at the outlet at the lower boundary

$$f(t) = q(L,T) \quad 23$$

Further the pressure head  $g(t)$  is measured at the upper boundary:

$$g(t) = h(0,t)$$

24

The physical properties of the experiments allow us to assure that it suffices to describe the flow in the column by the Richards equation in one spatial dimension. Solving the model for given hydraulic functions  $\theta$  and  $K$  and assigning the measurements  $f(t)$  and  $g(t)$  to  $\theta$  and  $K$  characterize the direct problem. The inverse problem consists of determining the hydraulic functions  $\theta$  and  $K$  from given measurements  $f(t)$  and  $g(t)$ . In general the inverse problem is ill-posed; therefore it is necessary to appropriate a regularization strategy for stable solution.



### **3 Literature Review**

### 3.1 Experimental Methods

Jiri Siminek and co-workers (1999) performed infiltration experiments on a loamy soil in the laboratory for the purpose of estimating the unsaturated hydraulic properties. The soil was packed in a soil container with tensiometers arranged along the column at different depths and was exposed to natural rainfall conditions. A time domain reflectometer was installed at a required depth to measure the water content. Soil hydraulic parameters were estimated and combined with numerical solution of the Richards equation to estimate the unsaturated hydraulic conductivity (Jiri Siminek et al 1999).

Another experimental procedure was used by Schaap et al (2003) on soil samples collected from boreholes at a site and taken to the laboratory to determine the unsaturated hydraulic conductivity of the soil. The soil sample was kept in column with porous plate on the bottom and connected to a graduated cylinder with a pressure transducer to measure the water level. The column at the top was connected to a pressure regulator that allowed air pressure ranging from 0 to 1 bar to be applied (Schaap et al 2003). The sample was saturated and air pressure increased in periodic increments and measurements were taken for each individual applied pressure. Every pressure increase drives water out of sample, through the porous plate at the bottom into the burette where the time-series of the outflow volume was recorded with a pressure transducer. When the flow stops, static equilibrium exists and at this point the water retention was determined. The final water content was determined by drying the samples at 105 C. This measurement also yielded

the bulk density of the sample. Saturated hydraulic conductivity was determined with the constant head method, after the samples were used in the multi-step outflow method. Hydraulic parameters were optimized using non-linear regression fit and unsaturated hydraulic conductivities of the samples were determined using van Genuchten and Mualem model (Schaap et al 2003).

### **3.1.1 Determining the hydraulic conductivity of the soil by means of field scale drainage model**

A field scale drainage model experiment was developed for sandy soil by Severino and co-workers (2003). Neutron probes were installed at different locations to measure the water content at different depths. Tensiometers were installed at the same locations to measure the pressure head at these depths. After completion of field measurements, soil samples were taken to the laboratory to determine the soil hydraulic parameters. Least-squares optimization procedure using Levenberg-Marquardt algorithm was used to estimate the parameters and hydraulic conductivity was determined using the data obtained from the field and laboratory (Severino et al 2003).

### **3.1.2 Analysis of Unsaturated water flow in a large sand tank**

Britta Schmalz and co-workers (2003) conducted an experiment in a large sand tank filled with Columbia silt loam to determine the soil water relation in unsaturated zone. The unsaturated soil hydraulic properties were described using Van Genuchten-Mualem type expressions. Infiltration experiments were carried out using a large tank contained

three sloped sidewalls. The tank was filled with a layer of homogeneous sand. Measurements of the pressure head were taken using two vertical tensiometers and the water content using time domain reflectometer at eight different depths. The lower boundary was separated into five compartments to obtain information about the spatial variability of the discharge rate. Calculations were performed using adaptive time stepping and boundary conditions (van Genuchten et al 2000). These experiments were performed on different types of soils and hydraulic parameters were identified and listed in Table 1. The hydraulic parameters residual water content  $\theta_r$ , saturated water content  $\theta_s$ , inverse air entry value  $\alpha$ , pore-size distribution index  $n$ , and saturated hydraulic conductivity  $K_s$  were used in determining the unsaturated hydraulic conductivity (van Genuchten et al 2000).

Table 1 Average Values of Van Genuchten Model soil hydraulic parameters for major soil textural groups according to (Van Genuchten, 2000)

Texture	$\theta_r$ [cm <sup>3</sup> /cm <sup>3</sup> ]	$\theta_s$ [cm <sup>3</sup> /cm <sup>3</sup> ]	$\alpha$ [1/cm]	$n$ [-]	<b>Ks</b> [cm/day]
Sand	0.043	0.43	0.145	2.68	712.80
Loamy Sand	0.057	0.410	0.124	2.28	350.20
Sandy Loam	0.065	0.410	0.075	1.89	106.10
Loam	0.078	0.430	0.036	1.56	24.96
Silt	0.034	0.460	0.016	1.37	6.00
Silt Loam	0.067	0.450	0.020	1.41	10.80
Sandy Clay Loam	0.100	0.390	0.059	1.48	31.44
Clay Loam	0.095	0.410	0.019	1.31	6.24
Silty Clay Loam	0.089	0.430	0.010	1.23	1.68
Sandy Clay	0.100	0.380	0.027	1.23	2.88
Silty Clay	0.070	0.360	0.005	1.09	0.48
Clay	0.068	0.380	0.008	1.09	4.80

### 3.2 Parameter estimation

The Brooks and Corey equation (equation 14) is one of the most important empirical equations in determining the hydraulic properties. This equation was modified by van Genuchten for more accurate description of observed soil hydraulic data near saturation, especially for undisturbed and many fine textured soils. Van Genuchten

predicted  $K(h)$  as a function of  $\theta(h)$  obtained with one of the statistical pore size distribution model because hydraulic conductivity is extremely sensitive to small changes in shape retention curve near saturation. The difference between the predicted  $K(h)$  obtained from both Brooks Corey and Van Genuchten models shows extreme non linearity for fine textured soils and less severe for coarse textured soils (van Genuchten 1980)

### **3.2.1 Predicting unsaturated hydraulic conductivity of porous media based on the physical properties**

The combination of non-similar media concepts to the one-parameter Brooks and Corey model has been used to predict unsaturated hydraulic conductivity of various soils (Zhuang et al, 2001). The theory of non-similar media concept consists of parameters characterizing the soil physical variability available and to incorporate these into existing models. The unsaturated hydraulic conductivity involves different parameters, which are obtained through correlating water retention curve to hydraulic conductivity curve of specific soil samples. The input parameters are soil bulk density, particle size distribution, soil water retention characteristics and saturated hydraulic conductivity. The methods generally used for estimating the unsaturated hydraulic conductivity are confounded by the complex pore characteristic, which usually results in non-homogeneous velocity field of water flow and in turn includes variability of soil hydraulic properties.

More than 50 soils with textures ranging from sand to clay were selected from the hydraulic database and used with different models. This non-similar media concept has yielded accurate results when compared to other models such as Brooks-Corey model, Van Genuchten and other models (Zhaung et al, 2001).

The saturated hydraulic conductivity was calculated from the grain-size distribution of the sand according to the Hazen relationship (1996) (Britta Schmalz et al 2003):

$$K_s = 41.76(d_{10})^2 \quad 25$$

Where  $K_s$  is the saturated hydraulic conductivity and  $d_{10}$  is the diameter of the soil particles at 10% of the cumulative grain size distribution.

The grain size distribution was measured every 10 cm along the vertical profile as well as horizontal profiles. The mean bulk density was measured at different depths. Soil water retention functions were obtained from the pressure head and water content data measurements taken in the sand tank during infiltration experiments. The methods of estimating the soil hydraulic parameters assume  $\theta_r$  and  $\theta_s$  are held constant. For this purpose  $\theta_r$  was set equal to 0 and  $\theta_s$  was set equal to porosity as calculated from the bulk density at each depth and the particle density using the equation:

$$\phi = 1 - \rho_b \rho_s^{-1} \quad 26$$

Where  $\phi$  is the porosity,  $\rho_b$  is the bulk density and  $\rho_s$  the particle density.

The mean flux was computed for the five outflow compartments. The discharge rates were distributed relatively uniformly along the lower boundary for all the simulation runs, with slightly higher fluxes in the middle of the tank and along the portions of the sidewalls. The analysis of this experiment concludes that the selected optimization procedures produced different water retention parameter sets. The saturated water content  $\theta_s$  was estimated the most critical factor affecting all other soil hydraulic parameters. In contrast, observed variabilities in the discharge rate with time is reasonable with an average water retention curve using porosity for  $\theta_s$ . This scenario produced more realistic range in the measured water contents (Britta Schmalz et al 2003).

### **3.2.2 Assessment of the hydraulic characteristics of unsaturated base-course materials**

The measurement of soil water characteristics over a full range of matric suction for well graded compacted granular materials requires large representative samples and time-consuming laboratory experimentation. The samples were compacted and arranged in layers at the optimum modified proctor conditions in a high mold. This mold was instrumented with tensiometers to measure the matric suction and time domain reflectometer probes to measure the water content at different levels. The tensiometers measure the negative pressure pore-water pressure in the soil surrounding the probe. Since the samples were tested at atmospheric pressure, pore-air pressure is equal to zero and the matric suction ( $h = p_a - p_w$ ) is  $h = -p_w$ . The tensiometers were made with high air entry ceramic cups with an air entry value of 100 kPa, which is maximum sustainable



matrix suction. The time domain reflectometer probes were composed of three stainless steel rods with a spacing of 2 cm. A cable tester was used to send an electromagnetic wave down a coaxial cable into the probe. The signal received by the tester is used to determine the dielectric constant of the material, which is related to the volumetric water content using specific calibration curves for all materials (Cote et al 1997).

The hydraulic conductivities for nearly saturated samples were obtained from constant head permeability tests, at a controlled temperature. The samples were compacted using modified optimum proctor water content and subjected to a constant head flow of de-aired water in the vertical direction. Saturated hydraulic conductivity was calculated using Darcy's Law.

The flow of water in compacted granular materials takes place through a complex network of the interconnected pores, the size and dispersion of which depend on many factors, such as degree of compaction and stability of the base-course materials. The porosity of such well-graded materials is thus greatly affected by fine content.

The porosity of the coarse grained soil can be computed as

$$\phi_c = \frac{V_t - V_{sc}}{V_t} \quad 27$$

where  $V_t$  is the total volume occupied by the soil,  $V_{sc}$  is the volume of the voids in the coarse grained soil

Porosity of the fine fraction is obtained as  $\phi_f$

$$\phi_f = \left[ \frac{V_t - V_s}{V_t} \right] \left[ \frac{V_t}{V_t - V_{sc}} \right] = \frac{\phi}{\phi_c} \quad 28$$

The soil hydraulic parameters have the influence on the fine fraction porosity as well as surface area of the fines fraction. Firstly, air entry value was related to both the porosity and the fines content. When the air entry ( $h_a$ ) value is plotted against the fines fraction porosity a relationship is obtained from the graph. The exponential relationship between  $h_a$  and  $\phi_f$  is best expressed as:

$$\log h_a = 3.92 - 5.19\phi_f \quad 29$$

The pore size distribution index  $n$  can be related to specific surface area of the samples  $S_{sf}$ . The experimental function  $n$  as a function of  $S_{sf}$  and  $\phi_f$  is

$$n = 0.385 - 0.021\phi_f^{0.65} S_{sf} \quad 30$$

The hydraulic conductivity of the soil depends on many factors like degree of saturation, porosity and others. The comparison of hydraulic conductivity values must be done for unique degree of saturation, which is usually set for 100%. The saturated values of hydraulic conductivity were extrapolated from the experimental degree of saturation achieved for hydraulic conductivity measurements. The relationship of saturated hydraulic conductivity can be expressed as

$$\log(K_s S_{sf}) = 9.94n_f - 12.64 \quad 31$$

The saturated water content  $\theta_s$ , which is equal to  $100n$ , the basic hydraulic parameters needed for calculating hydraulic conductivity were determined. The unsaturated hydraulic conductivity of the soil was determined using the Brooks –Corey and Van Genuchten Models (Cote et al, 1997).

### 3.2.3 Parameter Estimation and Identifiability Analysis

The van Genuchten (VG) curve and the Brooks Corey (BC) Curve were fitted to the static water retention data using non-linear optimization. The objective function that was minimized as (J. Simunek 1998)

$$\phi(b, \theta) = \sum_{i=1}^{N_{\theta}} [\theta^*(h_i) - \theta(h_i, b)]^2 \quad 32$$

Where  $N_{\theta}$  is the number of static retention measurements,  $\theta^*(h_i)$  is the water content for measurement  $i$  at a pressure head of  $h_i$ ,  $\theta(h_i, b)$  is the water content estimate by the VG or the BC equation, and  $b$  is the parameter vector consisting of  $\theta_r, \theta_s, \alpha$  and  $n$

### 3.2.4 Inverse determination of unsaturated hydraulic parameters

After determining the hydraulic properties particle-size distribution of the sample was measured using wet sieving. The particle size fractions were summarized into different fractions and analyzed by log-linear interpolation.

Parameter optimization is an indirect approach for the estimation of soil hydraulic parameters for the transient flow. Inverse methods are typically based upon the minimization of a suitable objective function, which expresses the discrepancy between the observed values and the predicted system response. Soil hydraulic properties are assumed to describe an analytical model with unknown parameter values.

The objective function  $\phi$  to be minimized during the parameter estimation process may be defined as (Simunek 1998)

$$\begin{aligned} \phi(b, q, p) = & \sum_{j=1}^{m_q} v_j \sum_{i=1}^{n_{qj}} w_{i,j} [q_j^*(x, t_i) - q_j(x, t_i, b)]^2 + \\ & \sum_{j=1}^{m_p} v_j \sum_{i=1}^{n_{pj}} w_{i,j} [p_j^*(\theta_i) - p_j(\theta_i, b)]^2 + \sum_{j=1}^{n_b} v_j [b_j^* - b_j]^2 \end{aligned} \quad 33$$

where the first term on the right hand side represents deviations between the measured and calculated space-time variables. In this term  $m_q$  is the number of different sets of measurements at the time  $t_i$  for the  $j^{\text{th}}$  measurements set at location  $x(r, z)$ ,  $q_j(x, t_i, b)$  are the corresponding model predictions for the vector of optimized parameters  $b$  and  $v_j$  and  $w_{i,j}$  are the weights associated with a particular measurement set respectively. The second term of equation 33 represents the difference between independently measured and predicted soil hydraulic properties and hydraulic conductivity. The last term represents a penalty function for derivations between prior knowledge of soil hydraulic parameters and their final estimates.

The inverse solution produces a correlation matrix, which specifies degree of correlation between the fitted coefficients. The correlation matrix quantifies changes in model predictions caused by small changes in the final estimate of a particular parameter, relative to similar changes as a result of change in the other parameters. The correlation matrix reflects nonorthogonality between two parameter values (Simunek 1998).

An important measure of the goodness of fit is the  $r^2$  value for the regression of the observed,  $y_i$  versus the fitted  $y_i(b)$ , values (J. Simunek 1998),

$$r^2 = \frac{\left[ \sum w_i \bar{y}_i y_i - \frac{\sum \bar{y}_i \sum y_i}{\sum w_i} \right]}{\left[ \sum w_i \bar{y}_i^2 - \frac{(\sum \bar{y}_i)^2}{\sum w_i} \right] \left[ \sum y_i^2 - \frac{(\sum y_i)^2}{\sum w_i} \right]} \quad 34$$

The  $r^2$  is the measure of the relative magnitude of the total sum of squares associated with the fitted equation. This solution provides the upper and lower bounds of the 95% confidence level around each fitted parameter.

## **4 Conductivity of Porous Media – Considering HLW Salt Cake**

The saltcake has porous nature similar to that of soil. The properties of soil-water mixtures under saturated and unsaturated conditions have been extensively studied and theoretical and experimental data are available (Schaap et al, 2002). It is assumed that the wettability of the brine solution on the surface of the salt crystals will be similar to soil-water relationship in the vadose zone and the same theoretical concepts will apply to the modeling of the hydraulic properties of saltcake.

#### **4.1 Multiphase Flow in Porous Media**

The partially saturated zone is a multiphase system, consisting of three phases: the solid phase of the soil matrix (or saltcake), gaseous and water phases. The unsaturated zone has solid and fluid properties defined over the porous media continuum and are based on mass conservation laws applied to each fluid phase present. The combination of mass balance equations and appropriate constitutive equations results in a set equations for the multi-phase unsaturated-zone system. To define these equations, the following are the assumptions made (Binning, 1994):

- Three phases are assumed to be present in the system: solid, liquid and gas phases. The solid phase is assumed to be immobile and consolidated. The gas and liquid phases are assumed to be fully mobile, but are assumed to be immiscible.
- Problems will be considered on the time scale of a single infiltration event and so evaporation is assumed to be negligible. For longer time scales water vapor transport is an important mechanism of water movement and consolidation can alter the porous material properties.

- The media is assumed to be isothermal. Heat is an important variable in mass transfer between phases but is neglected here.
- The porous media assumed to have different sizes of averaging volumes centered at a point i.e., representative elementary volume (REV).
- The flow is assumed to be laminar and it follows the Darcy's law.

The saturation profile created after drainage results from a balancing of the gravitational and capillary forces. Gravitational forces act to pull water downward, while capillary forces act to retain water in the medium. Initially under free drainage, gravitational forces dominate and water drains under unit gradient. As the water in the soil drains to lower horizons the water content decreases and the capillary pressure increases. Eventually, the gradient in the capillary forces equally oppose the gradient in the gravitational forces and the water will be at equilibrium causing the drainage to cease (Dicarlo et al, 2003). As the high level waste or the saltcake in SRS tanks has a porous nature, the relationship between moisture content and the pressure head in the saltcake is calculated using the correlations developed for soil by van Genuchten (1980).



## **5 Materials and Methods**

The experimental setup used in this study consisted of a column of height 40 cm and diameter of 30 cm with an inlet for nitrogen gas and an outlet for the collection of drained interstitial fluid. Two tensiometers were installed along the column to measure the pressure head at different depths. At the inlet a pressure valve was connected to control and measure the inlet pressure. The drained interstitial fluid at the outlet is collected in a beaker that is kept on a weighing balance to monitor the weight of the solution with time. The following are the major instruments that were used in this experiment.

## **5.1 Equipment**

### **5.1.1 Tensiometer**

The tensiometer used consists of a vacuum gauge connected with a tube to a porous ceramic tip. The tube is filled with water and is normally transparent so the water level within it can easily be seen. The ceramic tip is permeable, and the water in the tube saturates it. The tip is placed in contact with the saltcake in the column. As water moves from the tube into the saltcake, a partial vacuum is created and measured by the gauge. This measurement is not a direct measurement of saltcake water content. Rather, it is a measurement of saltcake water tension. The tensiometer reading is accurate as long as air does not enter the tube, so the system must remain hydrated. Unlike water, air readily expands and contracts as pressure changes, and therefore air in the tensiometer tube causes inaccurate measurements. Even if the instrument does not have any leaks, air dissolved in the water will accumulate during normal operation. This air must be removed periodically by refilling the tensiometer with water to restore reliable operation.

The tensiometer is connected to a current transducer. This is one of the most accurate means of converting soil moisture tension measurements into a continuous analog output. Figure 1 and Figure 2 show pictures of the tensiometer connected to a pressure transducer.

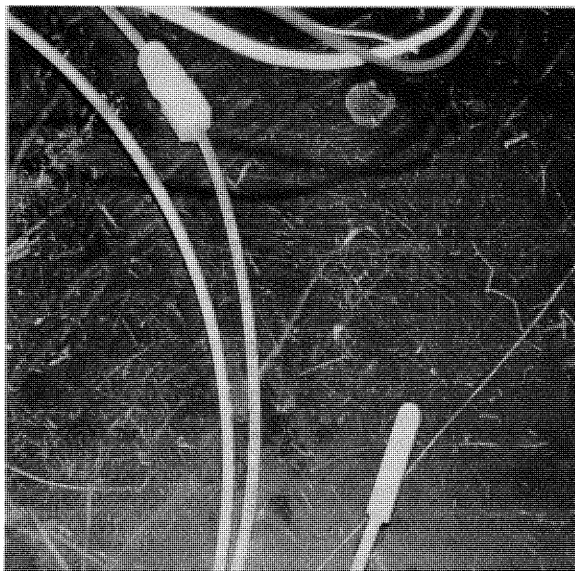


Figure 1 Tensiometer with Ceramic Porous cup

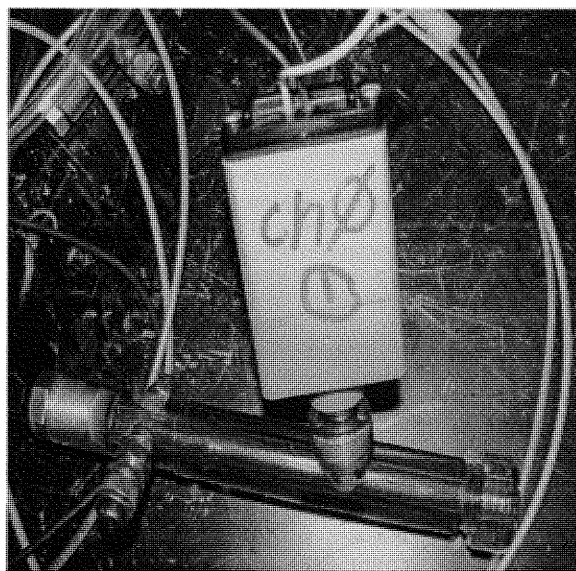


Figure 2 Pressure transducer

### 5.1.2 Pressure Transducer

The Model 5301 current transducer (Soil Moisture Equipment Corp., Santa Barbara, CA) is one of the most advanced, versatile, accurate means of converting the pressure head measurements to analog output. The standard current transducer incorporates 0 to 1 bar range transducer and solid-state circuitry, which allows continuous monitoring of the soil moisture suction time. When mounting the current transducer the threads on the connection stem of the transducer line up with the threads in

the plastic body tube of the tensiometer so that they enter easily. The current transducer is screwed in the clockwise direction until the backup washer on the stem touches the body of the tube and then the current transducer is unscrewed a portion of a turn until the top of case is facing up. To verify the tensiometer or transducer assembly is working properly first, dip the ceramic sensing tip of the tensiometer in water to fill the pores with water and seal off entry of air. Leave the tip in water for a minute or two and remove the tensiometer cap and support the tensiometer so that the vacuum hand pump can be inserted at the top of the unit. Connect the DC power source to the power leads of the current transducer and an ammeter to the output. When no vacuum is applied, the ammeter should read 4 mA and this is the calibration checkpoint. The 12 to 40 V DC power supply is connected to the power lead wires and an ammeter or data logger connected to the output wires of the computer. All the data from the tensiometers were recorded in the data acquisition system loaded on the computer. Figure 3 provides a sketch of the tensiometers attached to the pressure transducer and data acquisition system.

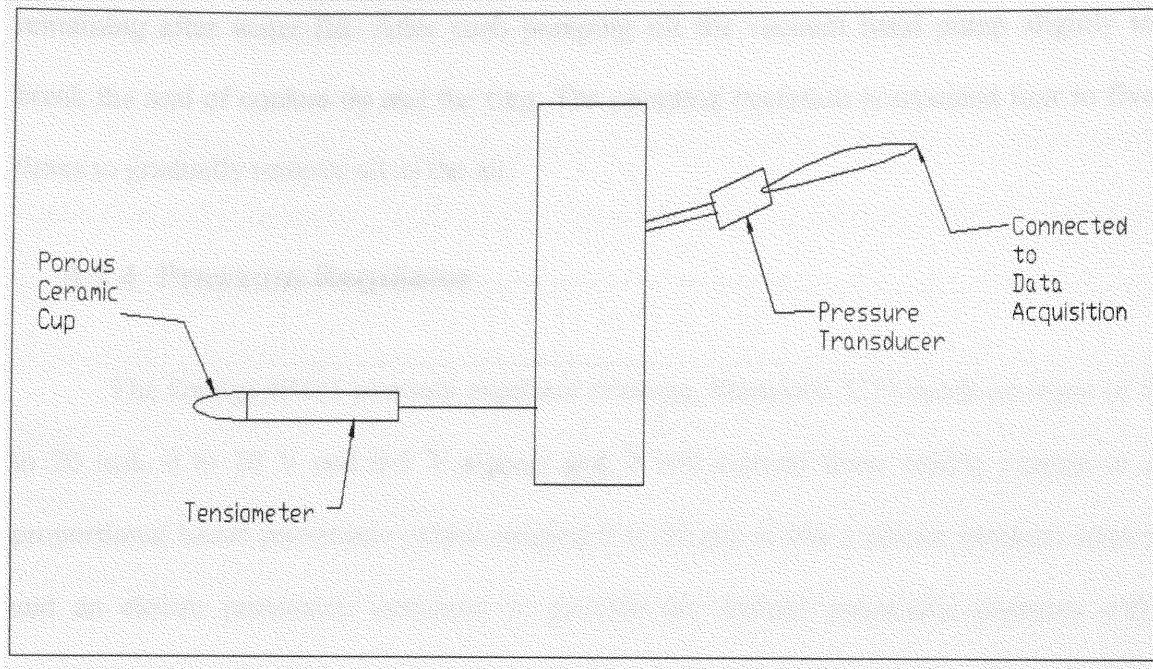


Figure 3 Tensiometer attached to the pressure transducer

### 5.1.3 Vacuum Hand Pump

The vacuum pump model 2005G1 (Soil Moisture Equipment Corp., Santa Barbara CA) supplies a source of vacuum for the soil water samplers and portable extractor. This pump contains inlet valve and outlet valve so that continuous pumping is accomplished with each stroke of the handle. Air or other fluids are pulled in at the tip end and exhausted to the side through the fitting at the opposite end of the pump. A maximum vacuum of 90 centibars can be obtained. The conical rubber tip on the end of the vacuum hand pump is inserted into the filler end of the tensiometer body. The conical tip held firmly against the cap seal in the body to create a seal. As the pump handle is pulled out, suction will be created within the tensiometer to expand the air bubbles

remaining after water fill. After each pumping tilt the vacuum hand pump slightly to break the seal of conical tip and the ring. The pumping operation is repeated four to five times to gradually remove all of the air.

#### 5.1.4 Pressure Regulator

The Omega IP411 pressure regulator (Omega, Stamford, CT) needs an input of 4 to 20 mA, 0 to 10 V and 0-5 V signals and it will convert these analog signals to a proportional linear pneumatic output ranging 0 to 20 psi. It has a silicon pressure sensor and an electro pneumatic converter to provide the desired pneumatic pressure with constant air consumption. Figure 4 and Figure 5 are the photographs of the pressure controller and the data acquisition hardware.



Figure 4 Pressure Controller

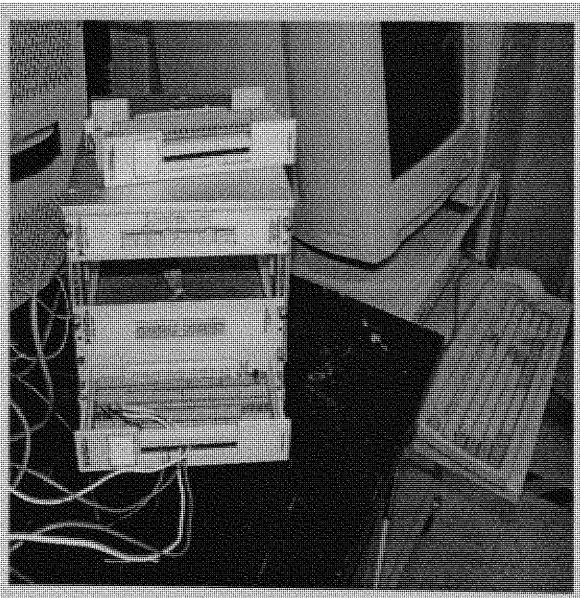


Figure 5 National Instruments data acquisition hardware

## 5.2 Data Acquisition

The data acquisition consists of three modules SCXI 1303, SCXI 1180, SCXI 1124 (National Instruments, Austin, TX). These three were connected with the pressure transducers to record the pressure head in the column and also connected to the pressure controller as output to maintain the specified pressure in the column. The data acquisition system is connected to a PC which has the software Labview (National Instruments, Austin, TX) installed in it. This Labview stores the data of pressure head based on the time interval that was selected

The SCXI terminal blocks (National Instruments, Austin, TX) provide direct connections to transducers at the screw terminal block located with full enclosure. This block is especially designed for high accuracy thermo couple measurements, includes isothermal construction that minimizes errors caused by thermal gradients between the terminals. The SCXI 1124 is six channel-isolated source for static DC voltage or current signals and 12 bit digital analog converter channels. It can be configured each channel for voltage or current output. Each channel output ranges from 0 to 20 mA. This module is software configurable program with each channel for voltage output ranges such as 0 to 10V (National Instruments Handbook). The terminal blocks are interconnected and finally connected to a computer. The pressure head data will be recorded on a timely basis in the computer.

## 5.3 Saltbed Simulant Preparation

### 5.3.1 Saltcake composition

Saltcake simulant was prepared using different varieties of sodium salts. The estimated amount of salts were calculated based on the actual saltcake sample (minus the radioactive components) sample amount and the estimated values used are listed in Table2

Table 2 Saltcake simulant chemicals

Chemical	Estimated Amount, kg
Sodium Aluminate	6.112
Sodium Hydroxide	2.641
Sodium Carbonate	6.566
Sodium Oxalate	0.139
Sodium Phosphate	1.130
Sodium Sulphate	0.946
Sodium Chloride	0.029
Sodium Nitrite	1.284
Sodium Nitrate	43.001
Water	88.041
Total	149.890
Less evaporate	49.890
GOAL	100.000



### 5.3.2 Steps in preparation of the saltcake simulant

1. A mixer and three band heaters were placed in a 30-gallon (136L) tank labeled “Batch 1”. The tare weight (tank, mixer, and heater) was recorded on the Data Sheet.
2. Deionized water was added to the tank until it was half-filled. The tank was placed on a hot plate. A thermometer was added to the water to monitor the temperature.
3. 7.322 kg of sodium aluminate ( $\text{NaAlO}_2$ ) was weighed using small beaker. Sodium aluminate was added slowly to the water.
4. The sodium aluminate solution was heated to 50–60°C. 3.164 kg of sodium hydroxide ( $\text{NaOH}$ ) as solid pellets was added slowly and carefully. The remainder of the chemicals was added in the order shown below. After each addition, the solution was stirred long enough to allow the solid to dissolve. The heaters were adjusted at 50°C throughout the reagent addition.
  - 7.867 kg sodium carbonate ( $\text{Na}_2\text{CO}_3$ )
  - 0.167 kg sodium oxalate ( $\text{Na}_2\text{C}_2\text{O}_4$ )
  - 1.354 kg sodium phosphate dodecahydrate ( $\text{Na}_3\text{PO}_4 \cdot 12\text{H}_2\text{O} \cdot 0.25\text{NaOH}$ )
  - 1.134 kg sodium sulfate ( $\text{Na}_2\text{SO}_4$ )
  - 35 g sodium chloride ( $\text{NaCl}$ )
  - 1.538 kg sodium nitrite ( $\text{NaNO}_2$ )
  - 51.515 kg sodium nitrate ( $\text{NaNO}_3$ )

5. The solution was allowed to evaporate. The goal of the evaporation and cooling portion of the procedure is to produce saltcake slurry that contains approximately 5-10% supernatant liquid after settling at ambient temperature.

Figure 6 shows the picture of the experimental setup with all the components.

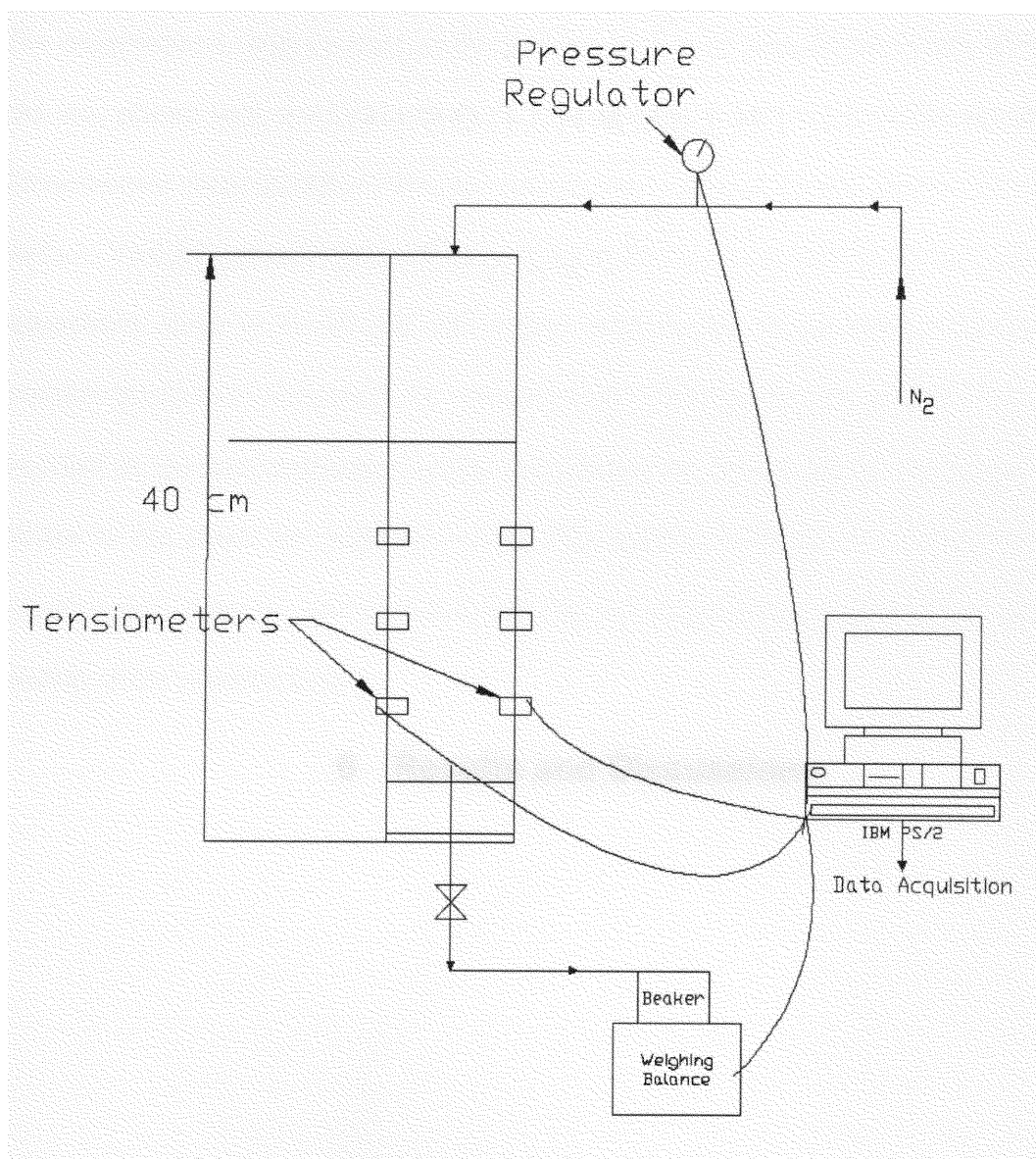


Figure 6 Experimental Setup

## **6 Results and Discussions**

## 6.1 Pressure Head

The experimental setup consists of 40 cm long column of with 30 cm length of saltcake and was placed with two tensiometers to measure the pressure head inside the saltcake. Tensiometers were installed with the porous cup centered 1 inch above the saltcake surface. Variable pressure boundary conditions of 100, 200 and 500 cm were applied in consecutive steps at 0, 20 and 107 hours, respectively. Tensiometers attached with pressure transducers measured the pressure head. Readings of the pressure head were recorded in the data acquisition system and plotted vs. time as shown in Figure 7. The values in the graph are negative because the applied pressure is in the direction of negative axis. Average measurement from the two tensiometers was taken as the actual reading of the pressure head.

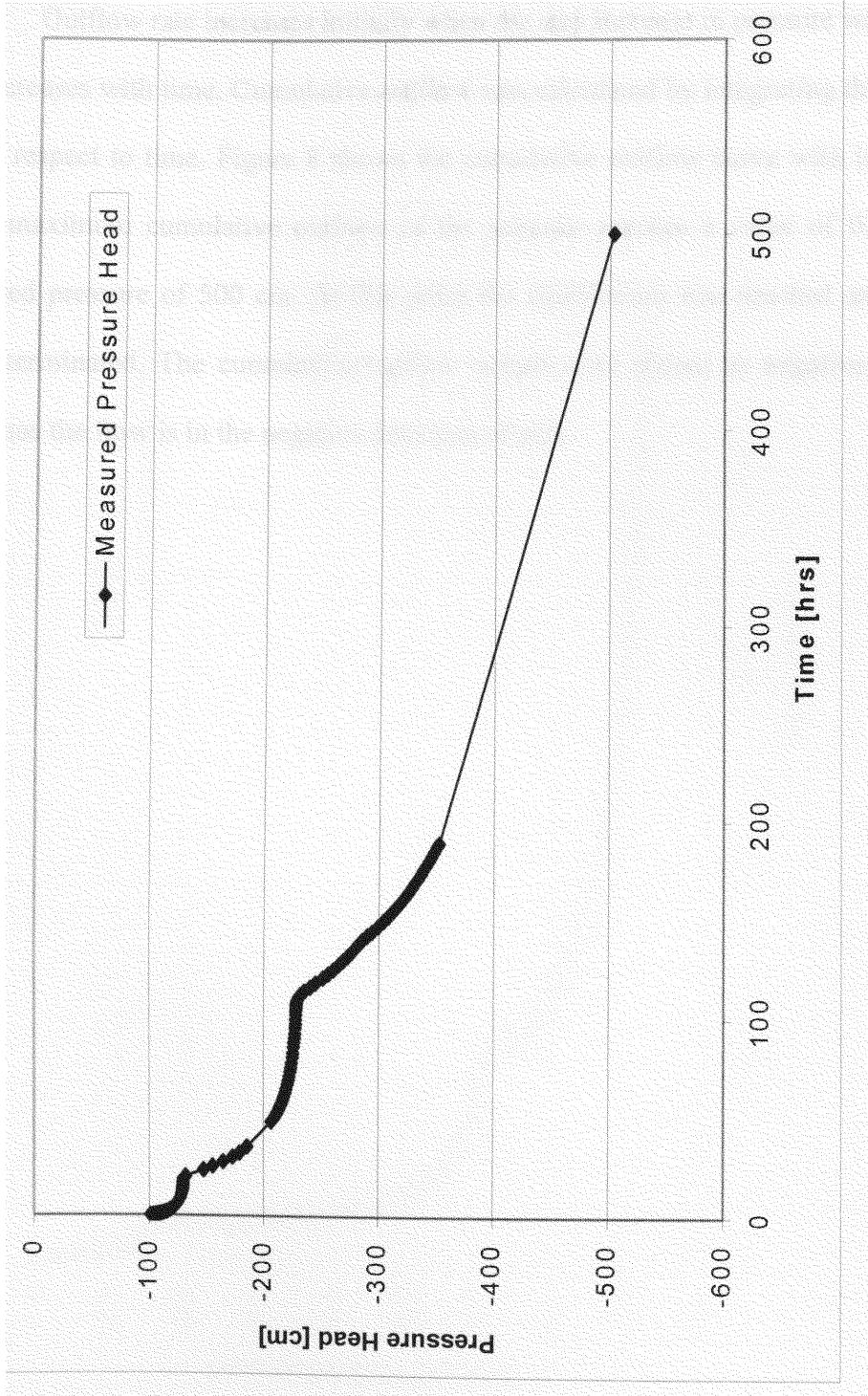


Figure 7 Measured cumulative bottom flux

## 6.2 Cumulative Outflow

Outflow rate increases initially when the step increase in pressure was applied and it decreases with time. Cumulative outflow was calculated by integrating the outflow rate with respect to time. Figure 8 shows the cumulative outflow curve with increased flux. The maximum cumulative outflow of the saltcake reaches a value of 0.81 cm at the applied pressure of 500 cm. At this point the equilibrium was reached and experiment was terminated. The cumulative outflow values were shown as negative in the graph because the flow is in the negative direction of axis.

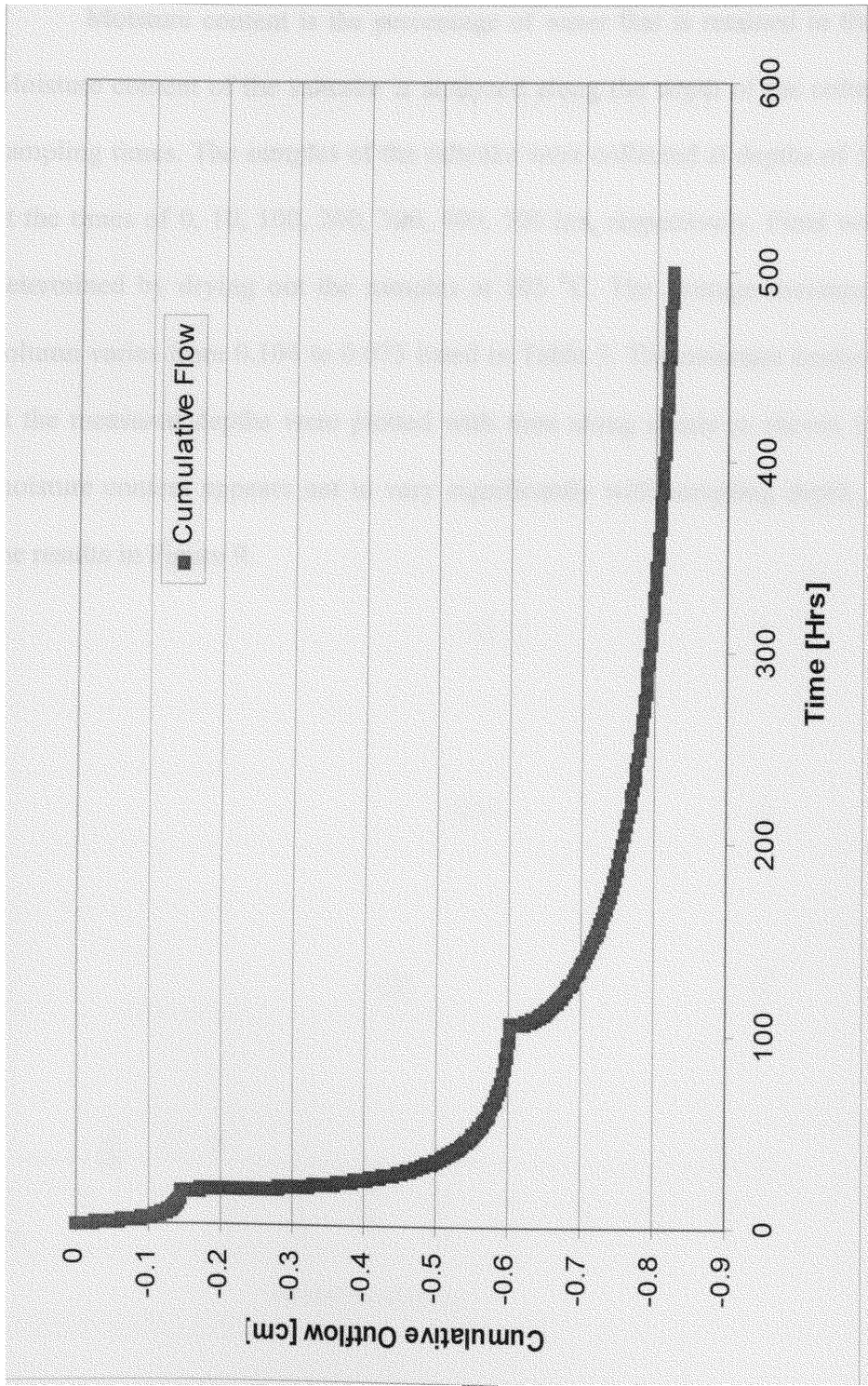


Figure 8 Comparison of outflow rate and cumulative outflow



### 6.3 Moisture content

Moisture content is the percentage of water that is retained in the porous media. Moisture content of the saltcake is analyzed along the depth of the column for different sampling times. The samples of the saltcake were collected at depths of 5, 15, 30 cm and at the times of 0, 10, 100, 200, 300, 400, 500 hrs, respectively. Final water content was determined by drying out the samples at 105 °C. The average moisture content in the column varies from 0.104 to 0.075 listed in Table 3. The moisture content in the column at the measured depths were plotted with time along x-axis as shown in Figure 9. The moisture content appears not to vary significantly with sampling depth, as indicated by the results in Figure 9.

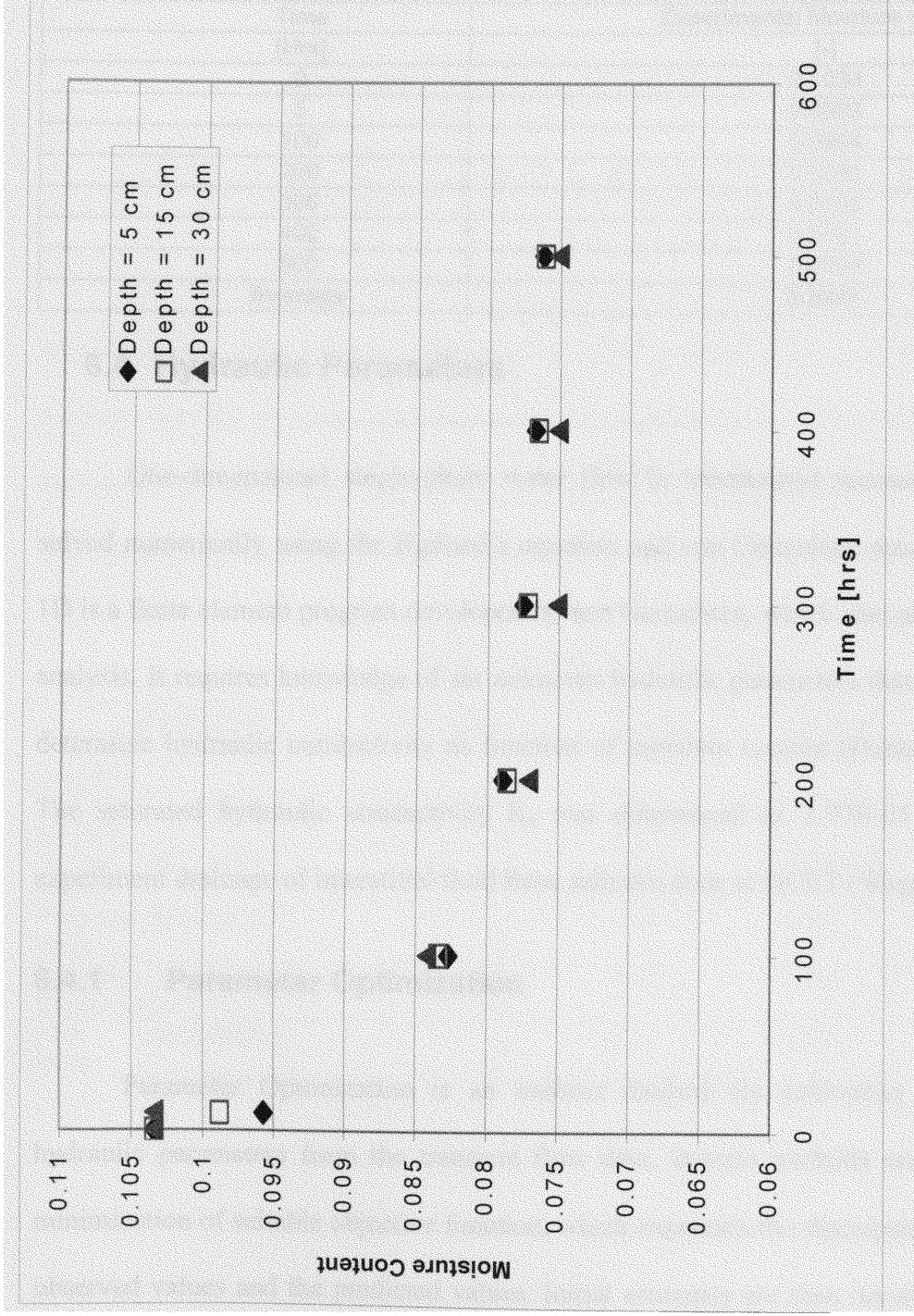


Figure 9 Moisture content variation with time

Table 3 Average moisture content obtained from the experimental data

Time [Hrs]	Experimental Moisture Content [-]
0	0.1034
5	0.0993
100	0.0834
200	0.0782
300	0.0766
400	0.0761
500	0.0758
<b>Average</b>	<b>0.0847</b>

## 6.4 Hydraulic Parameters

One-dimensional single-phase water flow in unsaturated porous media can be solved numerically using the Richard's equation and van Genuchten models. HYDRUS 1D is a finite element program developed by van Genuchten, which also performs inverse analysis. It requires knowledge of six unknown hydraulic parameters that can be used to determine hydraulic conductivity as function of moisture content (Durner et al, 1999). The saturated hydraulic conductivity  $K_s$  was determined as  $2.77E-03$  m/s from the experiment drainage of interstitial fluid from saltcake done at HCET (Weger et al, 2003)

### 6.4.1 Parameter Optimization

Parameter Optimization is an indirect method for estimating porous media hydraulic parameters from the transient flow data. Inverse methods are based on the minimization of suitable objective function, which expresses the discrepancy between the observed values and the predicted values. Initial estimates are then iteratively improved during the minimization process until a value precision is obtained. The objective

function to be minimized during the parameter optimization is defined as (Simunek et al 2000):

$$\phi(b, q, p) = \sum_{j=1}^{m_q} v_j \sum_{i=1}^{n_{qj}} w_{i,j} [q_j^*(x, t_i) - q_j(x, t_i, b)]^2 + \sum_{j=1}^{m_p} v_j \sum_{i=1}^{n_{pj}} w_{i,j} [p_j^*(\theta_i) - p_j(\theta_i, b)]^2 + \sum_{j=1}^{n_b} v_j [b_j^* - b_j]^2 \quad 35$$

The minimization of the objective function is accomplished by using nonlinear regression fit. This method combines descend methods and generates confidence intervals for the optimized parameters (van Genuchten et al 1980) Table 4 shows the estimated and optimized parameters. The error was calculated between two parameters. The optimized parameters were estimated at 95 percent confidence limits.

Table 4 Comparison of parameters

Description	Parameter	Direct	Inverse	Units
Residual Water Content	$\theta_r$	0.065	0.071	[cm <sup>3</sup> /cm <sup>3</sup> ]
Saturated water content	$\theta_s$	0.41	0.3765	[cm <sup>3</sup> /cm <sup>3</sup> ]
Inverse air entry value	$\alpha$	0.075	0.05204	[1/cm]
Pore-size distribution index	$n$	1.89	2.36	[-]
Saturated Hydraulic Conductivity	$K_s$	1000	1000	[cm/hr]
Pore connectivity factor	$l$	0.5	0.55	[-]

## 6.5 Hydraulic Conductivity

The measured values of pressure head from the tensiometer readings, moisture content from the samples, and outflow from the column were used to calculate the hydraulic conductivity of the saltcake using van Genuchten model. The van Genuchten parameters  $\theta_r, \theta_s, \alpha, l, n, K_s$  are obtained from the HYDRUS-1D software. Saturated hydraulic conductivity was set to 2.77E-03 m/s in order to provide best fit for other parameters listed in Table 4. Unsaturated hydraulic conductivity along the depth of the column was calculated using HYDRUS software direct simulation.

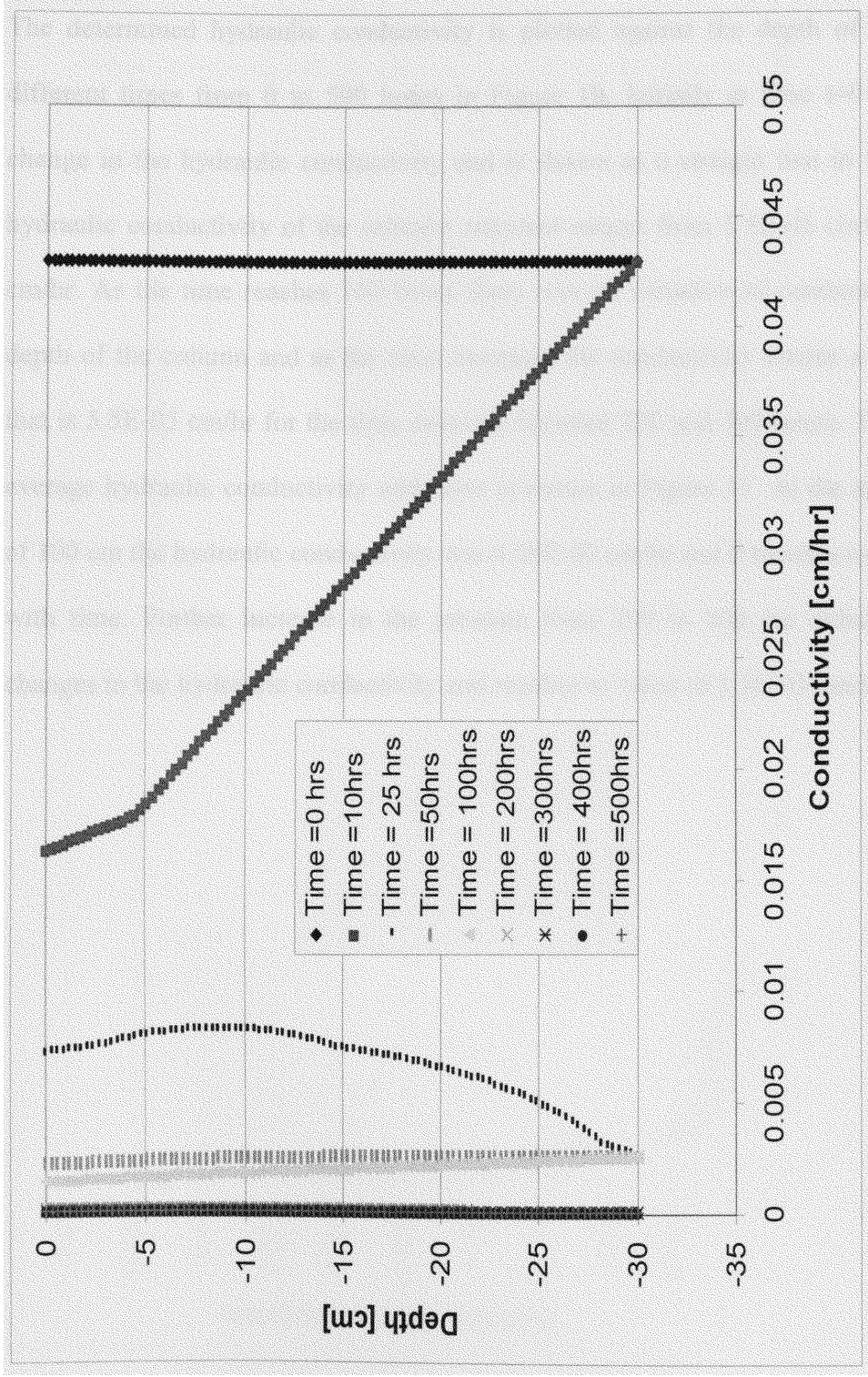


Figure 10 Variation of Hydraulic conductivity with time

The determined hydraulic conductivity is plotted against the depth of the column at different times from 0 to 500 hours in Figure 10. Initially at time  $t=0$  hr there is no change in the hydraulic conductivity and is shown as a straight line in Figure 10. The hydraulic conductivity of the saltcake simulant ranges from  $5.5E-05$  cm/hr to  $4.29E-02$  cm/hr. As the time reaches 100 hours there was no variation of conductivity along the depth of the column and as the time increases the conductivity attains a constant value that is  $5.5E-05$  cm/hr for the time intervals between 200 and 500 hours. The variation of average hydraulic conductivity with time is shown in Figure 11. At the applied pressure of 100 cm the hydraulic conductivity was  $4.29E-02$  cm/hr and it reaches to  $1.2E-02$  cm/hr with time. Further increase in the pressure from 200 to 500 cm indicates the minor changes in the hydraulic conductivity and reaches to value of  $5.5E-05$  cm/hr.

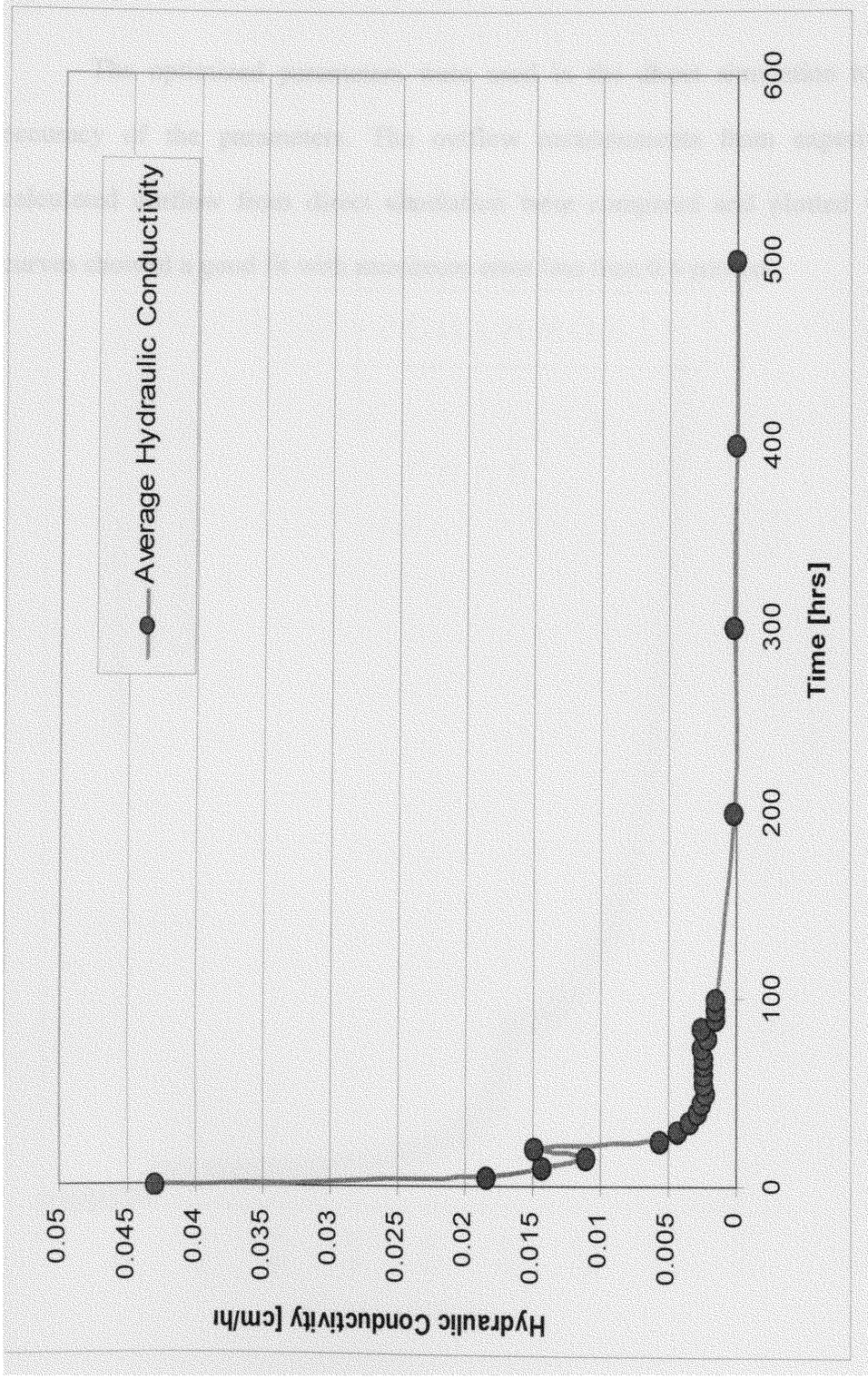


Figure 11 Variation of average hydraulic conductivity with time



## **6.6 Direct analysis using inverse optimized parameters**

The optimized parameters were used in the direct simulation to compare the accuracy of the parameters. The outflow measurements from experiment and the calculated outflow from direct simulation were compared and plotted vs. time. Two curves showed a good fit with maximum error less than 0.6 percent.

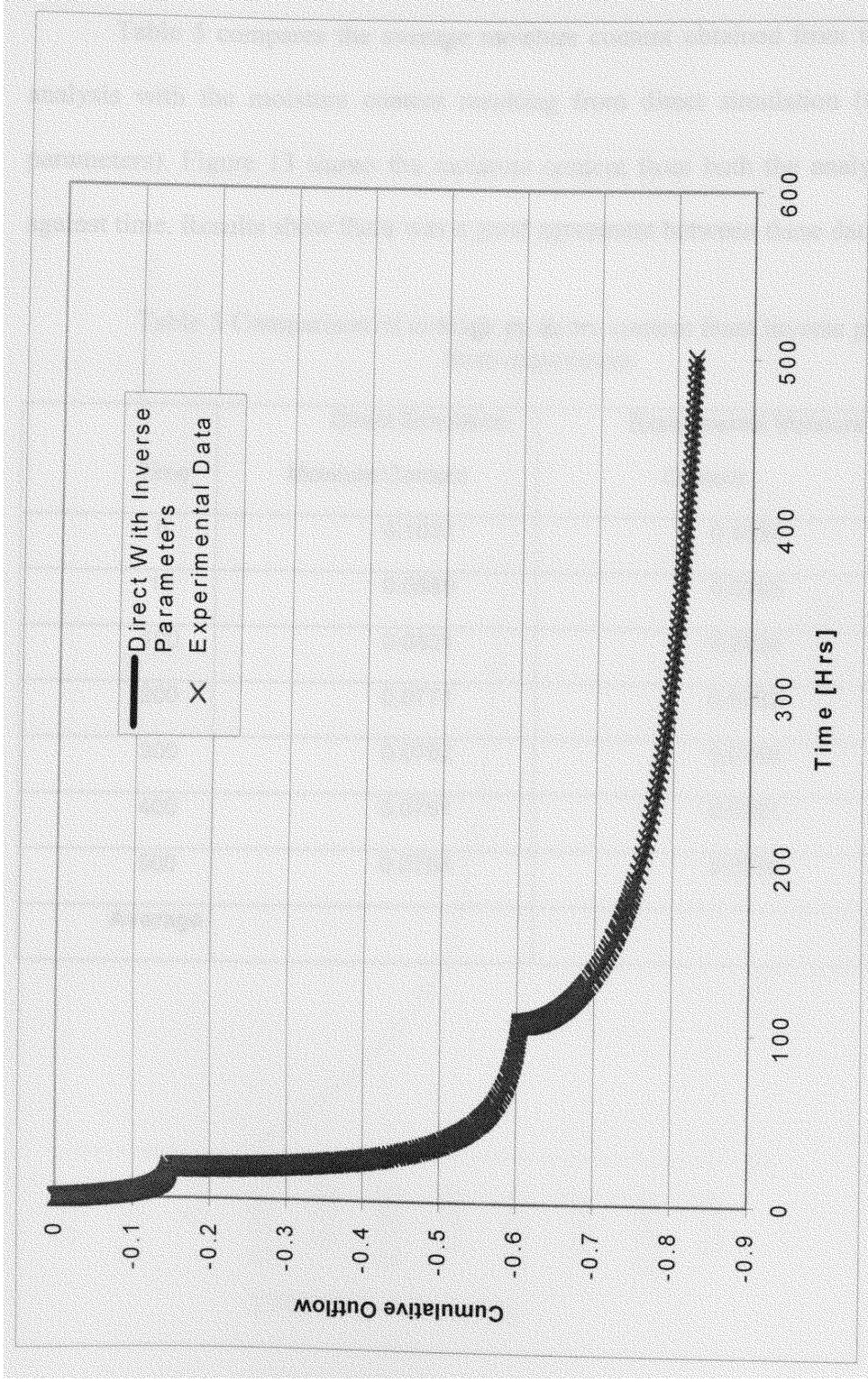


Figure 12 Cumulative Outflow comparison of direct analysis with inverse parameters with inverse analysis

Table 5 compares the average moisture content obtained from the experimental analysis with the moisture content resulting from direct simulation (using optimized parameters). Figure 13 shows the moisture content from both the analyses was plotted against time. Results show there was a good agreement between these data.

Table 5 Comparison of average moisture content from inverse parameters and from experiment

Time	Direct Simulation Moisture Content	Experimental Moisture Content	% Difference
0	0.1031	0.1034	0.2901
10	0.0989	0.0993	0.3693
100	0.0831	0.0834	0.4395
200	0.0771	0.0782	1.3640
300	0.0762	0.0766	0.5222
400	0.0757	0.0761	0.5256
500	0.0754	0.0758	0.5277
<b>Average</b>			<b>0.5769 %</b>

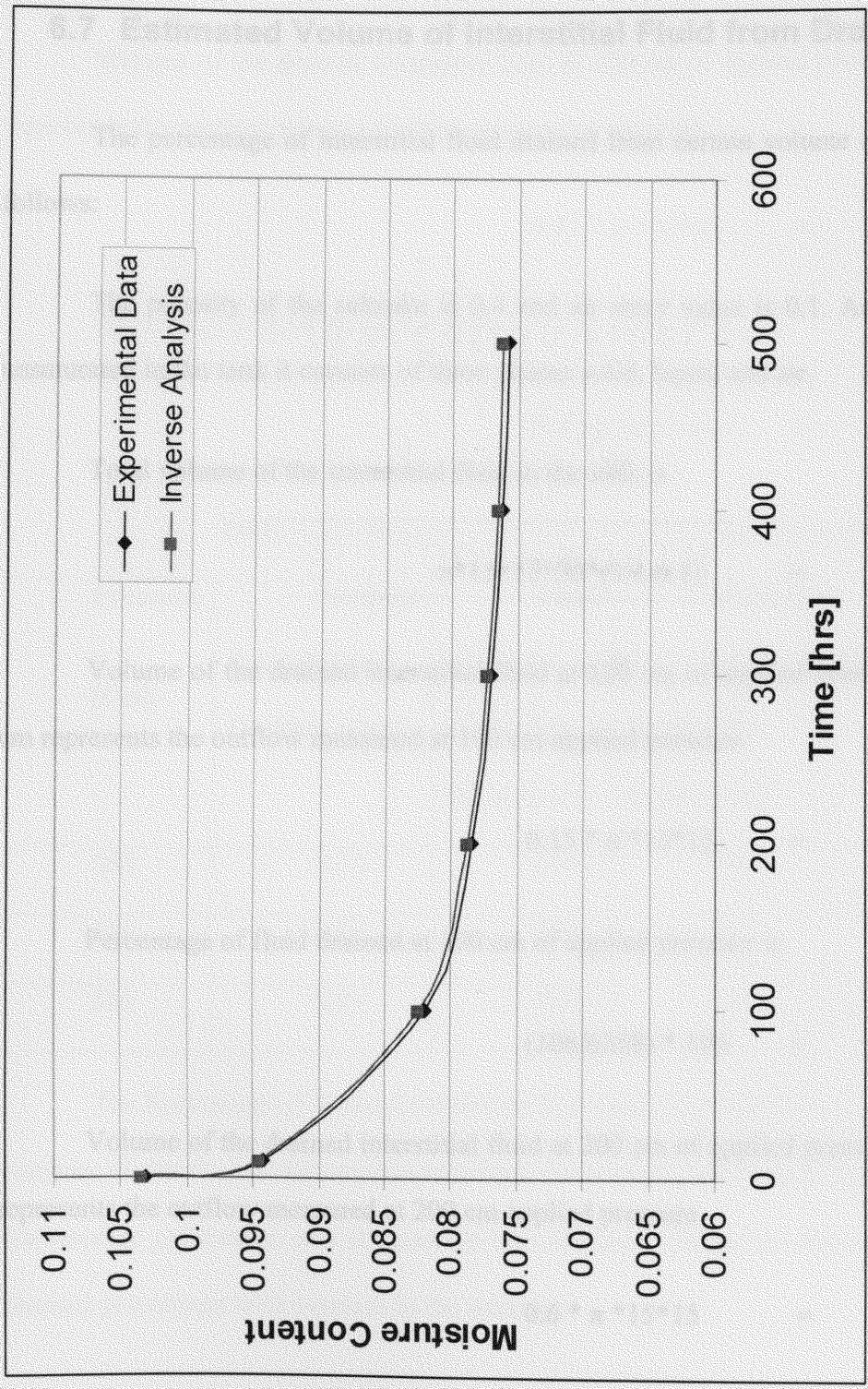


Figure 13 Moisture content comparison from Experimental and inverse analysis

## 6.7 Estimated Volume of Interstitial Fluid from Drainage

The percentage of interstitial fluid drained from certain volume of saltcake is as follows:

The porosity of the saltcake is 0.4 and air entry value is 0.1. As the saltcake is unsaturated in the tank it consists of three phases solid, liquid and air.

Total volume of the interstitial fluid in the tank is

$$\pi * 15 * 15 * 30 * (0.4 - 0.1) = 6358 \text{ cm}^3$$

Volume of the drained interstitial fluid at 100 cm of applied pressure where 0.15 cm represents the outflow measured at 100 cm applied pressure

$$0.15 * \pi * 15 * 15 = 106 \text{ cm}^3$$

Percentage of fluid drained at 100 cm of applied pressure is

$$(106/6358) * 100 = 2.0 \%$$

Volume of the drained interstitial fluid at 200 cm of applied pressure where 0.6 is represents the outflow measured at 200 cm applied pressure

$$0.6 * \pi * 15 * 15 = 424 \text{ cm}^3$$

Percentage of fluid drained at 200 cm of applied pressure is

$$(424/6358) * 100 = 6.6 \%$$

Volume of the drained interstitial fluid at 500 cm of applied pressure where 0.81 represents the outflow measured at 500 cm applied pressure

$$0.81 * \pi * 15 * 15 = 573 \text{ cm}^3$$

Percentage of fluid drained at 500 cm of applied pressure is

$$(573/6358) * 100 = 9.0 \%$$

Table 6 Percentages of drained interstitial fluid from the tank

<b>Pressure [Cm]</b>	<b>Average Cumulative Outflow [Cm]</b>	<b>Total Volume of interstitial Fluid [Cm<sup>3</sup>]</b>	<b>Volume of Drained Interstitial Fluid [Cm<sup>3</sup>]</b>	<b>Percentage Drained [%]</b>
100	0.15	6358	106	2.0
200	0.6	6358	424	6.6
500	0.81	6358	573	9.0

The Percentage of drained interstitial fluid was calculated for each step increase in pressure (Table 6). For the experimental tank the drained percentages were calculated and the average percentage was six percent was obtained. Figure 14 shows the increase in drained percentage with increase in the pressure.

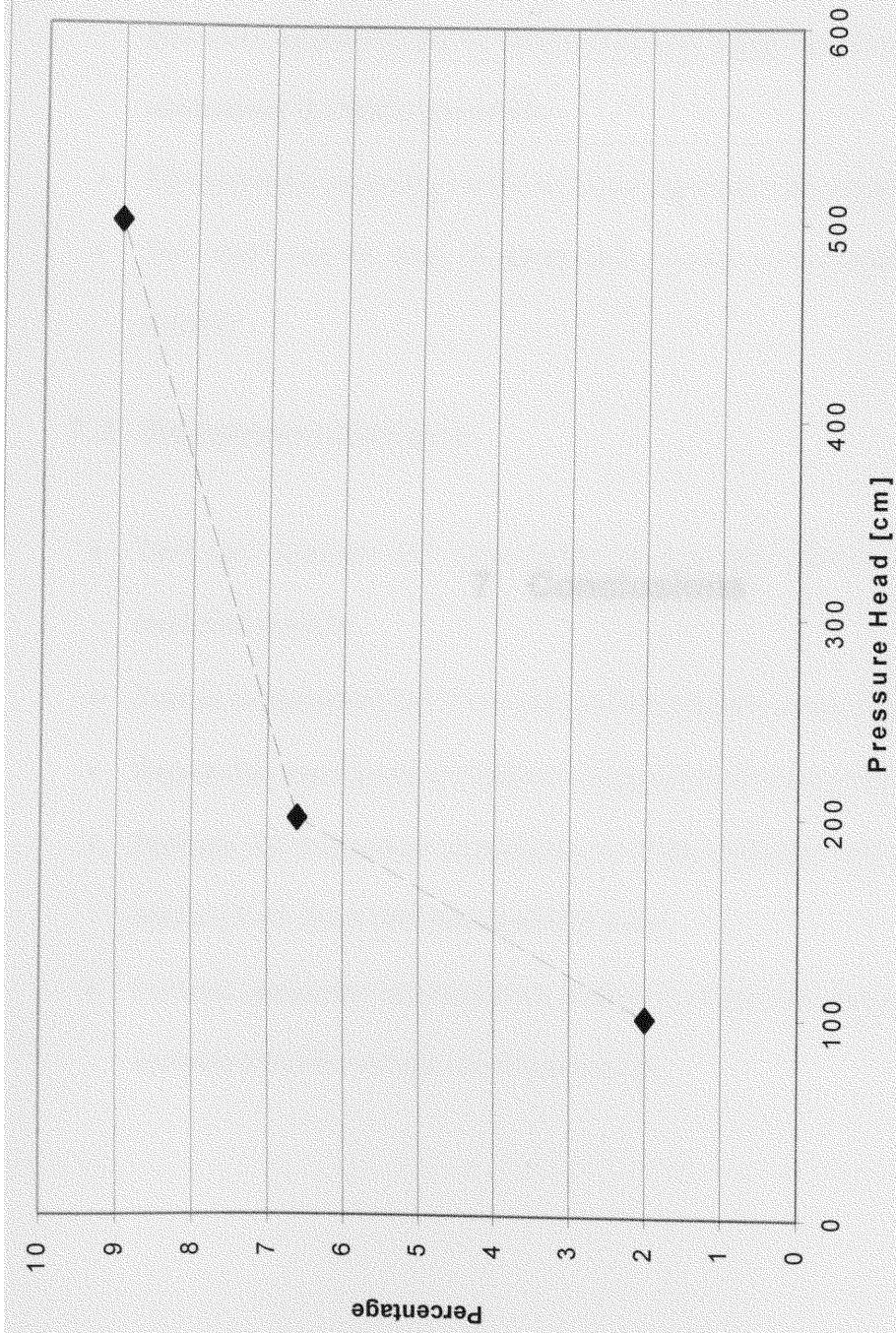


Figure 14 Increase of drainage percentage with increased pressure

## **7 Conclusions**



## 7.1 Conclusions

- This study showed that the high level waste simulant has hydraulic properties that were approximated to unsaturated soil using van Genuchten's model for unsaturated hydraulic properties.
- The hydraulic properties of the saltcake simulant were similar to the sandy loam
- This study can be used to predict the volume of interstitial fluid that can be drained

## 7.2 Recommendations

- Test and compare the using other models like Mualem, Van Genuchten's modified models.
- Run an independent test to validate estimated parameters for HLW
- Repeat this experiment for different high-level waste simulants
- Perform 3D Numerical Simulation of Tank drainage and compare with field results (T-41 from SRS has available data)
- Perform parameter identifiability studies to determine ranges for which inverse analysis provides unique set of parameters

## 8 References

A.RAMIREZ and W.DAILY, 1996. Detection of Leaks in Underground Storage Tanks Using Electrical Resistance Methods. U.S. Department of Energy, UCRL-ID-125918.

BOELS, D., van GILS, J.B.H.M., VEERMAN, G.J., & WIT, K.E., 1978. Theory and system of automatic determination of soil moisture characteristics and unsaturated hydraulic conductivities. *Soil Sci* 126: 191-199.

BRITTA SCHMALZ, BERND LENNARTZ and MARTINUS T. VAN GENUCHTEN, Analysis of unsaturated water flow in a large sand tank, *Soil Science*, 2003.

D.L NOYES and D.I.ALLEN, 2003. Integrated Mission Acceleration Plan, Prepared for U.S. Department of Energy. RPP-13678.

DAVID A. DICARLO, 2003. Drainage in finite-sized unsaturated zones. Agricultural Research Service

DURNER, W., 1994. Hydraulic conductivity estimation for soils with heterogeneous pore structure. *Water Resource Res* 30: 211-223

FEDDES, R.A., KABAT, P., van BAKEL, P.J.T., BRONSWIJK, J.J.B, & HALBERTSMA, J., 1988. Modeling soil water dynamics in the unsaturated zone - State of the art. *J Hydrology* 100: 69-111

GERADO SEVERINO, ALESSANDRO SANTINI, and ANGELO SOMMELLA, Determining the soil hydraulic conductivity by means of a field scale internal drainage, *Journal of hydrology*, 2003.

HALBERTSMA, J.M., & VEERMAN, G.J., 1994. A new calculation procedure and a simple set-up for the evaporation method to determine soil hydraulic functions. Report 88, SC-DLO, Wageningen, The Netherlands

ISO 11275 1996 Soil quality - Determination of the unsaturated hydraulic conductivity and water retention characteristic - Wind's evaporation method.

J. ZHUANG, K.NAKAYAMA, G.R. YU and T.MIYAZAKI, Predicting unsaturated hydraulic conductivity of soil based on some basic soil properties, *Soil & Tillage Research*, 2001.

J.COTE and J.M. KONRAD, Assessment of the hydraulic characteristics of unsaturated base-course materials: a practical method for pavement engineers, *Geotechnical Journal*, 2003.

J.N BROOKE, J.F. PETERS and K.STAHELL, 1999. Hydrological Methods can Separate Cesium from Nuclear Waste Saltcake. U.S. Department of Energy, WSRC-TR-99-00358.

J.SIMUNEK and M.TH VAN GENUCHTEN, The hydrus software packages for simulating water, heat and solute movement in this subsurface: Features, Recent Applications and Future Plans, Hydrologic Modeling Conference, 2002.

JIRI SIMUNEK, OLE WENDROTH, and MARTINUS T. VAN GENUCHTEN, Estimating unsaturated soil hydraulic properties from laboratory tension disc infiltrometer experiments, *Water Resources Research*, 1999.

JIRKA SIMUNEK, JAN W. HOPMANS, D.R. NIELSEN and M.TH. VAN GENUCHTEN, Horizontal infiltration revisited using parameter estimation, *Hydrology Program*, 2003.

M.GSCHAAP, P.J.SHOUSE and P.D.MEYER, 2003. Laboratory measurements of the unsaturated hydraulic properties at the vadose zone transport field study site, U.S. Department of Energy DE-AC06-76RL01830.

M.TH. VAN GENUCHTEN, 1980. A Closed form Equation for Predicting the Hydraulic Conductivity of Unsaturated Soils, *Soil Science Society American Journal* 44: 892-898.

MALICKI, M.A., PLAGGE, R., RENGER, M. & WALCZAK, R.T. 1992. Application of time-domain reflectometry (TDR) soil moisture miniprobe for the determination of unsaturated soil water characteristics from undisturbed soil cores. *Irrigation Science* 13: 65-72.

MARCEL G. SCHAAP, FEIKE J. LEIJ, and MARTINUS TH. VAN GENUCHTEN, Estimating the unsaturated soil hydraulic properties using a hierarchical set of pedotransfer functions, *Hydrologic Modeling Conference*, 2002.

P.C.SUUGS, The Savannah River Site Accelerated Clean-Up Mission: Salt Waste Disposal, U.S. Department of Energy, 2003.

STAHELI KIMBERLIE and HOHN F. PETERS, US Army Corps of Engineers, Waterways Experimental Station, Technical Report GL-98-3, April 1998.

STOLTE, J., FREYER, J.I., BOUTEN, W., DIRKSEN, C., HALBERTSMA, J.M., Van DAM, J.C., Van den BERG, J.A., VEERMAN, G.J. & WVSTEN, J.H.M. 1994. Comparison of six methods to determine unsaturated soil hydraulic conductivity. *Soil Science Soc Am J* 58: 1596-1603.

T.VOGEL, M.TH.VAN GENCUHTEN and M.CISLEROVA, Effect of the shape of the soil hydraulic functions near saturation on variably saturated flow predictions, *Advances in water resources*, 2001.

TAMARI, S., BRUCKLER, L., HALBERTSMA, J., & CHADOEUF, J. 1993. A simple method for determining soil hydraulic properties in the laboratory. *Soil Science Soc Am J* 57: 642-651

WENDROTH, O., EHLERS, W., HOPMANS, J.W., KAGE, H., HALBERTSMA, J. & WVSTEN, J.H.M. 1993. Re-evaluation of the evaporation method for determination of hydraulic functions in unsaturated soil. *Soil Science So Am J* 57: 1436-1443.

WIND, G.P. 1968. Capillary conductivity data estimated by a simple method. In: P.E. Rijtema and H. Wassink (editors), *Water in the unsaturated zone*, Proceedings of the Wageningen symposium, June 1966, IASH Gentbrugge/ Unesco Paris, Vol. 1, pp. 181-191